EPJ Web of Conferences **303**, 05004 (2024) https://doi.org/10.1051/epjconf/202430305004
MENU 2023

X17 discovery potential in $\gamma d \to e^+e^-pn$ at MAGIX@MESA

Cornelis J.G. Mommers[1,*] and *Marc* Vanderhaeghen[1]

[1]Institut für Kernphysik and PRISMA+ Cluster of Excellence, Johannes Gutenberg-Universität, D-55099 Mainz, Germany

Abstract. We propose a direct search experiment for X17 using deuteron photodisintegration, $\gamma d \to e^+e^-pn$, at the MAGIX@MESA experiment. X17 is a boson conjectured by the ATOMKI collaboration to explain anomalous signals around 17 MeV in excited ^{8}Be, ^{12}C and ^{4}He nuclear decays. It is the subject of an intense, global research program; an experiment at an electron accelerator would complement the ongoing effort to verify X17's existence. Using the plane-wave impulse approximation around the neutron quasi-free peak, we show that an enhanced X17 signal over the QED background is visible in $\gamma d \to e^+e^-pn$, assuming pseudoscalar, vector and axial-vector X17 scenarios. Additionally, we discuss how our calculation may be generalized to searches for a generic dark boson in a photon-deuteron reaction.

1 Introduction

While numerous observations corroborate the existence of dark matter, definitive proof of a new particle sector is still outstanding [1]. Traditionally, weakly-interactive massive particles have been the main paradigm in dark matter searches. In recent years, this focus has shifted towards light dark matter, sparking a renewed interest in low-energy, high-intensity experiments [2]. In view of the above, the potential discovery of a narrow resonance around 17 MeV by the ATOMKI collaboration – dubbed X17 – in the e^+e^- decay spectrum of excited states of ^{8}Be, ^{12}C and ^{4}He has garnered significant attention [3–6]. At present there are numerous ongoing or planned experimental efforts searching for X17. For a recent review, see Ref. [7].

Should X17 be a genuine new particle, it may be detected via Compton scattering off a nucleon. Unfortunately, conducting such a search is not entirely straightforward. Due to existing bounds, X17 might couple weakly to protons [8, 9]. Moreover, the lack of a free, high-density neutron target at accelerators means we cannot search for X17 in reactions such as $\gamma n \to e^+e^-n$ either. For this reason, we propose a direct search experiment for X17 using deuteron photodisintegration, $\gamma d \to e^+e^-pn$, with neutron tagging [10]. By tagging the outgoing neutron, one can treat the bound neutron as quasi-free and the bound proton as a spectator. In this way, scattering events take place primarily on the quasi-free neutron, and the reaction $\gamma n \to e^+e^-n$ is effectively probed by proxy. Our work is centered around a potential experiment at MAGIX@MESA [11], but can be readily adapted to meet the constraints provided by other electron scattering facilities.

*e-mail: cmommers@uni-mainz.de

MESA is a linear electron accelerator (presently under construction) that will be able to deliver a low-energy yet high intensity electron beam (up to 105 MeV in its energy-recovering mode) [11]. MAGIX@MESA is an experiment that will consist of two high-resolution spectrometers and a gas-jet target [12]. The spectrometers will be able to resolve the electron-positron invariant mass with a resolution of $\delta m_{ee} \approx 0.1$ MeV. Note that comparable resolutions have already been achieved in dark-photon searches at the A1 experiment at MAMI [13, 14].

As compared to other experiments, a direct search for X17 at MAGIX@MESA holds several advantages. First, such a search would disentangle X17's existence from possible unaccounted nuclear effects. Additionally, the data from MAGIX@MESA of the $\gamma d \to e^+e^-pn$ process would not only enable a search for X17, but also for any new boson with a mass between $\sim$ 10-100 MeV. This, in turn, would allow one to derive exclusion limits on the dark-matter neutron coupling (which are poorly constrained in this mass range [15, 16]). By combing the existing proton limits with the new neutron limits, one would be able to to derive limits on the effective dark-matter quark coupling, which would strongly restrict permissable new-physics models, such as the dark photon model (in which the neutron coupling must vanish). Therefore, a direct search for X17 at MAGIX@MESA would complement the ongoing experimental programs at other facilities.

2 $\gamma d \to e^+e^-pn$ amplitude in the plane-wave impulse approximation

2.1 Kinematics

We begin our calculation with the kinematics of the $\gamma d \to e^+e^-pn$ process. Throughout this work we give all quantities in the rest frame of the deuteron. We set up our coordinate system such that the z-axis is along the direction of the incoming photon three-momentum, and the neutron and photon three-momenta span the x-z plane. Then, we have

$$\gamma(E_\gamma, \mathbf{q}, \lambda)\, d(m_d, \mathbf{0}, M) \to e^+(E_+, \mathbf{p}_+, s_+)\, e^-(E_-, \mathbf{p}_-, s_-)\, p(E_p, \mathbf{p}_p, s_p)\, n(E_n, \mathbf{p}_n, s_n),$$

where λ is the polarization of the incoming photon, and $s_\pm$, s_p and s_n are $e^\pm$, p and n helicities, respectively, and M is the deuteron spin projection on the z-axis. The masses of the nucleons and deuteron are given by m_N and m_d, respectively. We denote the dilepton invariant mass as $m_{ee}^2 = q'^2$, with $q' = p_+ + p_-$ being the momenta of the virtual photon or X17. Our kinematic variables are E_γ, $|\mathbf{p}_\pm|$, the polar angles $\theta_\pm$ and θ_n, and the azimuthal angles $\phi_\pm$ and ϕ_n, where all polar angles are defined with respect to the z-axis. Using the shorthand $\mathrm{d}\Pi := \mathrm{d}|\mathbf{p}_+|\mathrm{d}|\mathbf{p}_-|\mathrm{d}\Omega_+\mathrm{d}\Omega_-\mathrm{d}\Omega_n$, the differential cross section is given by

$$\frac{\mathrm{d}\sigma}{\mathrm{d}\Pi} = \frac{1}{64(2\pi)^8 m_d E_\gamma} \frac{|\mathbf{p}_+|^2 |\mathbf{p}_-|^2}{E_+ E_-} \frac{|\mathbf{p}_n|^2}{|\mathbf{p}_n|(m_d + E_\gamma - q'^0) - E_n|\mathbf{q} - \mathbf{q}'| \cos\theta_{n\gamma\gamma}} \langle|\mathcal{M}|^2\rangle, \tag{1}$$

where $\langle|\mathcal{M}|^2\rangle$ is the spin-averaged squared matrix element. The angle $\theta_{n\gamma\gamma}$ is defined via

$$|\mathbf{q} - \mathbf{q}'| \cos\theta_{n\gamma\gamma} = (\mathbf{q} - \mathbf{q}') \cdot \mathbf{p}_n / |\mathbf{p}_n|. \tag{2}$$

2.2 The plane-wave impulse approximation around the neutron quasi-free peak

To compute $\mathcal{M}$ we work within the plane-wave impulse approximation (PWIA) [17], illustrated in Fig. 1. As we are interested in the low-energy regime, $E_\gamma \sim 100$ MeV, where relativistic corrections are expected to be small, we use a non-relativistic framework. We

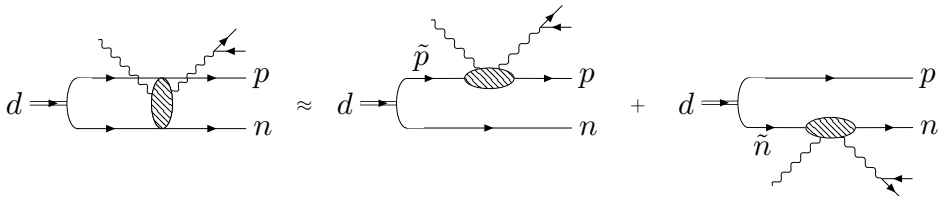

Figure 1. In the plane-wave impulse approximation we can factor $\gamma d \to e^+e^-pn$ into a process on a quasi-free neutron, $\tilde{n}$, and a quasi-free proton, $\tilde{p}$.

implement the PWIA by inserting a complete set of two-particle states,

$$\mathcal{M}_{\rm IA}(\gamma d \to e^+e^-pn) = \sum_{s_1,s_2}\int \frac{\mathrm{d}^3p}{2E_p(2\pi)^3}\,\langle e^+e^-,\ \mathbf{p}_p\,s_p,\ \mathbf{p}_n\,s_n\,|\,\mathcal{M}_{\rm IA}\,|\,\gamma,\ \tfrac{1}{2}\mathbf{p}_d+\mathbf{p}\,s_1,\ \tfrac{1}{2}\mathbf{p}_d-\mathbf{p}\,s_2\rangle$$
$$\times (2m_d)^{1/2}(2E_{\tilde{p}})^{1/2}(2E_{\tilde{n}})^{1/2}\,{}_{\rm NR}\langle \mathbf{p};\ s_1\,s_2\,|\,d(1,M)\rangle_{\rm NR}, \tag{3}$$

where 'NR' indicates the baryon states are normalized non-relativistically,

$$|\mathbf{p},\ s\rangle = (2E_p)^{1/2}|\mathbf{p},\ s\rangle_{\rm NR}, \quad \langle \mathbf{p},\ s\,|\,\mathbf{p}',\ s'\rangle = (2E_p)(2\pi)^3\delta^{(3)}(\mathbf{p}-\mathbf{p}')\delta_{ss'}.$$

In the second line of Eq. (3) we can identify the components of the relative deuteron wave function in momentum space, $\tilde{\Psi}^M_{s_1s_2}(\mathbf{p}) = {}_{\rm NR}\langle \mathbf{p};\ s_1\,s_2\,|\,d(1,M)\rangle_{\rm NR}$. Numerically, we use the CD-Bonn parametrization [18] for $\tilde{\Psi}$. We also restrict ourselves to the neutron quasi-free peak (NQFP), defined by [17]

$$|\mathbf{p}_p| \lesssim \sqrt{m_N\Delta} \approx 45.7\ \text{MeV/c}, \tag{4}$$

where $\Delta \approx 2.2$ MeV is the deuteron binding energy. In this kinematic regime we can ignore any contributions coming from scattering off the bound proton. Given that X17 may be protophobic, this restriction enhances our signal to background ratio.

Applying the PWIA in the NQFP simplifies the computation of $\mathrm{d}\sigma/\mathrm{d}\Pi$ to the computation of $\mathcal{M}(\gamma\tilde{n} \to e^+e^-n)$,

$$\mathcal{M}_{\rm IA}(\gamma d \to e^+e^-pn) \approx \mathcal{M}^{\rm n}_{\rm IA}(\gamma d \to e^+e^-pn) + \mathcal{M}^{\rm p}_{\rm IA}(\gamma d \to e^+e^-pn) \approx \mathcal{M}^{\rm n}_{\rm IA}(\gamma d \to e^+e^-pn), \tag{5}$$

with

$$\mathcal{M}^{\rm n}_{\rm IA}(\gamma d \to e^+e^-pn) = (2m_d)^{1/2}\left(\frac{E_p}{E_{\tilde{n}}}\right)^{1/2}\sum_{s_{\tilde{n}}}\tilde{\Psi}^M_{s_ps_{\tilde{n}}}\left(\mathbf{p}_p\right)\mathcal{M}\left(\gamma\,\tilde{n} \to e^+\,e^-\,n\right), \tag{6}$$

where in the *rhs* of Eq. (6) the quasi-free neutron has momentum and spin projection $-\mathbf{p}_p$ and $s_{\tilde{n}}$, respectively. Note, in Eq. (5) we disregard meson exchange currents and final-state interactions. In our kinematic regime of interest the meson exchange currents are estimated to give corrections of approximately 5% [17], meaning they can be safely neglected. Likewise, for a first approximation, the final state interactions can be omitted.

We now turn to the calculation of $\mathcal{M}(\gamma\,\tilde{n} \to e^+\,e^-\,n)$, which consists of two parts, the QED background and the X17 signal. We will begin with the QED background.

2.3 QED background processes and X17 signal processes

At E_γ around 100 MeV, the QED background may be parameterized by the combination of the Bethe-Heitler process and the Compton scattering process. In turn, the Compton scattering process consists of the Born and π^0 t-channel exchange contributions, as well as the non-Born contributions parameterized by the neutron electric and magnetic nucleon polarizabilities. These are all shown in Fig. 2, where crossed diagrams for the Bethe-Heitler and Born contributions have been omitted. All diagrams in Fig. 2 are to be embedded in the quasi-free neutron blob of Fig. 1.

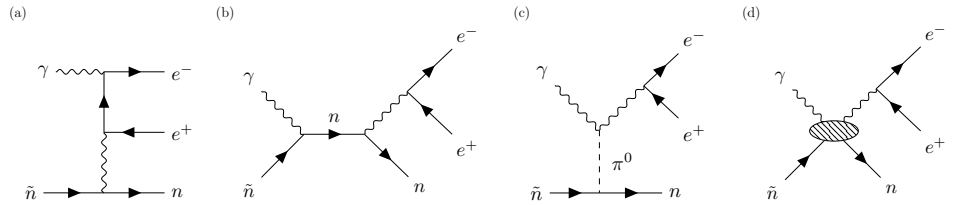

Figure 2. At $E_\gamma \sim 100$ MeV the reaction $\gamma\tilde{n} \to e^+e^-n$ is described by the Bethe-Heitler process (a), the Born process (b), π^0 t-channel exchange (c) and non-Born, neutron polarizability contributions (d). Crossed diagrams for the Bethe-Heitler and Born processes are not shown.

The X17 signal process is identical to Fig. 2b, with X17 replacing the virtual photon. In principle, X17 may also contribute via the Bethe-Heitler process. However, we only consider kinematics where X17 is on resonance in the Born process, meaning any Bethe-Heitler contributions with virtual X17 exchange are negligible and thus may safely be ignored.

From angular momentum and parity conservation it follows that X17 may be a pseudoscalar, vector or axial-vector particle. Accordingly, for the coupling of X17 to the nucleon we use models by Alves and Weiner [19] for the pseudoscalar case, by Feng *et al.* [9] for the vector case and by Kozaczuk *et al.* [20] for the axial-vector case,

$$\mathcal{L}_\mathrm{P} = i\bar{N}\gamma_5\left(g^{(0)}_{XNN} + g^{(1)}_{XNN}\tau_3\right)NX, \quad \mathcal{L}_\mathrm{V} = -eX_\mu \sum_{N=p,n} \varepsilon_N \bar{N}\gamma^\mu N, \quad \mathcal{L}_\mathrm{A} = -X_\mu \sum_{N=p,n} a_N \bar{N}\gamma^\mu\gamma_5 N, \tag{7}$$

where $e > 0$ is the proton charge, τ_3 is the isospin Pauli matrix, $g^{(0)}_{XNN}$ and $g^{(1)}_{XNN}$ the isoscalar and isovector pseudoscalar couplings, respectively, $\varepsilon_{p,n}$ the vector couplings and $a_{p,n}$ the axial-vector couplings.

The process of deriving explicit values for the coupling of X17 to the nucleons from the ATOMKI data is, by now, well-documented (see Refs. [9, 19–21], among others). We use the couplings derived in Ref. [10]. Note that currently there is an unresolved discrepancy between the X17 couplings derived from the beryllium and carbon measurements by the ATOMKI group. For completeness, we present each case separately. A comprehensive discussion on this apparent tension may be found in Refs. [10, 22, 23].

Lastly, the width of X17 is significantly smaller than MAGIX@MESA's m_{ee} bin width, δm_{ee} [3–6, 14]. This implies we may safely ignore any cross terms between the QED background and the X17 signal. It also means we should average the X17 signal over a single δm_{ee}-wide bin in the dilepton invariant mass,

$$\frac{\mathrm{d}\sigma}{\mathrm{d}\Pi} \approx \left(\frac{\mathrm{d}\sigma}{\mathrm{d}\Pi}\right)_\mathrm{QED} + \left(\overline{\frac{\mathrm{d}\sigma}{\mathrm{d}\Pi}}\right)_\mathrm{X17}, \quad \text{with} \quad \left(\overline{\frac{\mathrm{d}\sigma}{\mathrm{d}\Pi}}\right)_\mathrm{X17} := \frac{1}{\delta m_{ee}} \int_{m_X-\delta m_{ee}/2}^{m_X+\delta m_{ee}/2} \mathrm{d}m_{ee} \left(\frac{\mathrm{d}\sigma}{\mathrm{d}\Pi}\right)_\mathrm{X17}. \tag{8}$$

As a side effect this averaging procedure essentially washes away any dependence of the cross section on the coupling of X17 to the electron.

3 Results for the X17 signal around the neutron quasi-free peak

With all the ingredients to compute the cross section at hand, the remaining task is to optimize the kinematics for the highest signal to background ratio. When optimizing, we have to take the detector constraints of MAGIX@MESA setup into account. These limit [12]

$$20\ \text{MeV} \leq |\mathbf{p}_{\pm}|, \quad 15^\circ \leq \theta_{\pm} \leq 168^\circ, \quad 5^\circ \leq \theta_n \leq 175^\circ.$$

The final two constraints are that $m_X = m_{ee}$, so that we get a strong enhancement of the signal via the Born process, and the requirement that the NQFP condition 4 is satisfied. By scanning the available parameter range we found the optimal in-plane kinematics to be an asymmetric backward configuration for the lepton pair,

$$|\mathbf{p}_+| = 65.7\ \text{MeV/c}, \quad \theta_+ = -165.0^\circ, \quad |\mathbf{p}_-| = 20.1\ \text{MeV/c}, \quad \theta_- = 168.0^\circ, \quad \theta_n = 5.0^\circ,$$

where negative angles indicate that the positron is emitted in the opposite half plane compared to the electron and neutron. The NQFP corresponds to the angular range $\theta_n \in [-10, 18]$ °.

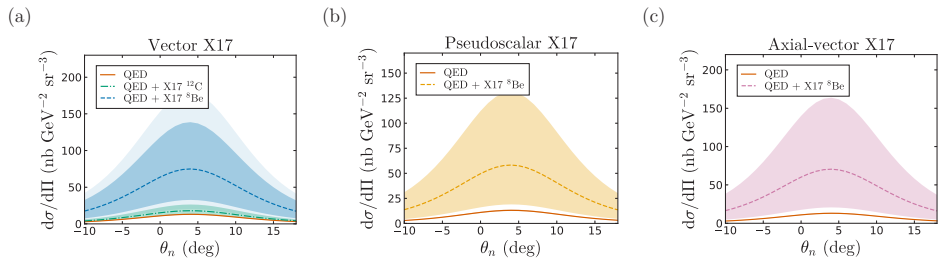

Figure 3. The differential cross section of $\gamma d \rightarrow e^+e^-pn$ using the plane-wave impulse approximation around the neutron quasi-free peak with optimum kinematics (see text), $E_\gamma = 105$ MeV, $m_X = m_{ee} = 17.02$ MeV and $\delta m_{ee} = 0.1$ MeV. (a) The dark and light blue (green) colors indicate 2σ and 3σ uncertainty ranges of the vector X17-^{8}Be (^{12}C) derived couplings, respectively. The yellow (b) and magenta (c) bands indicate 1σ uncertainty ranges in the ^{8}Be-derived couplings for a pseudoscalar or axial-vector X17, respectively. The red band indicates the uncertainty in the QED background due to the neutron polarizabilities

Figure 3(a) shows the differential cross section for a vector X17 as a function of θ_n. The blue and green signal curves use couplings derived from the beryllium and carbon data, respectively, and the dark and light bands represent 2σ and 3σ variations therein. Figures 3(b) and 3(c) show the pseudoscalar and axial-vector scenarios in yellow and magenta, respectively, with a 1σ variation in the coupling. In all cases the signal cross section is averaged over a bin of $\delta m_{ee} = 0.1$ MeV. The red QED background includes uncertainties from neutron polarizabilities as taken from the PDG [24]. We see that in all cases an X17-signal would be strongly enhanced over the QED background. In an experiment this enhancement would manifest itself as a single, sharply-peaked bin in m_{ee} spectrum. This is shown in Fig. 3(a) assuming a vector X17. A similar result holds for the pseudoscalar and axial-vector scenarios (not shown). In all cases the strong enhancement indicates discovery potential for X17.

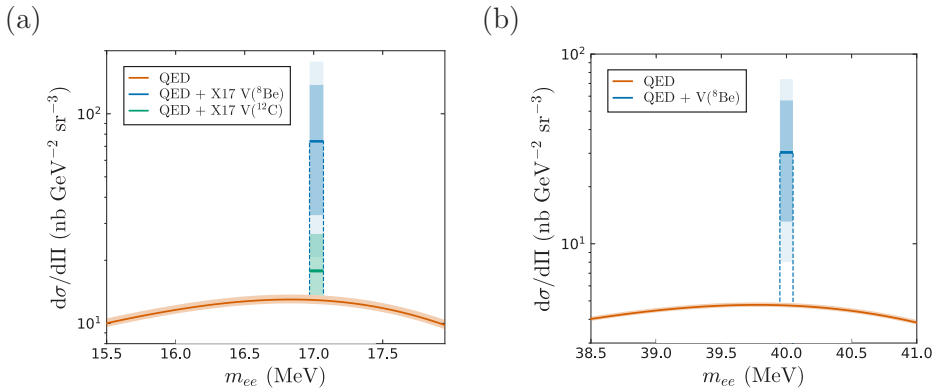

Figure 4. The signals of a vector X17 (a) or a hypothetical vector particle with a mass of 40 MeV (b) as they would appear inside a single bin with a width of 0.1 MeV where $E_\gamma = 105$ MeV, assuming optimal kinematics (see text). The colors carry the same meaning as in Fig. 3. m_{ee} is varied by varying $|\mathbf{p}_-|$.

In passing we note that one is not limited to X17, i.e. $m_{ee} = m_X \approx 17$ MeV. In the case of MAGIX@MESA, the spectrometers make the range $m_{ee} \in [5, 65]$ MeV kinematically accessible. Thus, by optimizing the kinematics assuming a different, fixed m_{ee} one can check for new bosons in the 5-65 MeV range. We give an example in Fig. 4, where we have assumed X17's ^{8}Be-derived couplings for simplicity. The signal of a new vector-like particle with a mass of 40 MeV appears as an enhanced peak, where the optimized in-plane kinematics are

$$|\mathbf{p}_+| = 49.5 \text{ MeV/c}, \quad \theta_+ = -168.0\,^\circ, \quad |\mathbf{p}_-| = 37.7 \text{ MeV/c}, \quad \theta_- = 136.9\,^\circ, \quad \theta_n = -5.0\,^\circ.$$

If one does not see signal, one can derive exclusion limits (see Ref. [25]) which, as previously mentioned, can be used to restrict new-physics models.

4 Summary and outlook

We have demonstrated that there is X17 discovery potential in a direct search experiment at MAGIX@MESA using the reaction $\gamma d \to e^+e^-pn$ with neutron tagging. On the experimental side, the next step would be a detailed simulation study. On the theoretical side, a further step is the inclusion of higher-order corrections in our calculation. Such developments may prove especially timely given that several independent X17 searches are ongoing. The addition of higher-order corrections also serves a dual purpose. It turns out that the kinematic regime in $\gamma d \to e^+e^-pn$ where one is sensitive to X17, is also the kinematic regime where one is most sensitive to the neutron polarizabilities. As the neutron polarizabilities are poorly determined [26], it is worthwhile to investigate whether they may also be extracted using the same data as from a dark matter search. Such extractions have previously been done using $\gamma d \to \gamma pn$ [17, 27] at MAMI.

This work was supported by the Deutsche Forschungsgemeinschaft (DFG, German Research Foundation), in part through the Research Unit [Photon-photon interactions in the Standard Model and beyond, Projektnummer 458854507 - FOR 5327], and in part through the Cluster of Excellence [Precision Physics, Fundamental Interactions, and Structure of Matter] (PRISMA$^+$ EXC 2118/1) within the German Excellence Strategy (Project ID 39083149).

References

[1] A. Arbey, F. Mahmoudi, Prog. Part. Nucl. Phys. **119**, 103865 (2021), 2104.11488
[2] G. Arcadi, M. Dutra, P. Ghosh, M. Lindner, Y. Mambrini, M. Pierre, S. Profumo, F.S. Queiroz, Eur. Phys. J. C **78**, 203 (2018), 1703.07364
[3] A.J. Krasznahorkay et al., Acta Phys. Polon. Supp. **8**, 597 (2015)
[4] A.J. Krasznahorkay, M. Csatlós, L. Csige, J. Gulyás, A. Krasznahorkay, B.M. Nyakó, I. Rajta, J. Timár, I. Vajda, N.J. Sas, Phys. Rev. C **104**, 044003 (2021)
[5] A.J. Krasznahorkay et al., Phys. Rev. C **106**, L061601 (2022)
[6] A.J. Krasznahorkay, A. Krasznahorkay, M. Csatlós, L. Csige, J. Timár, M. Begala, A. Krakó, I. Rajta, I. Vajda, (to be published) (2023), 2308.06473
[7] D.S.M. Alves et al., Eur. Phys. J. C **83**, 230 (2023)
[8] J.L. Feng, B. Fornal, I. Galon, S. Gardner, J. Smolinsky, T.M.P. Tait, P. Tanedo, Phys. Rev. Lett. **117**, 071803 (2016)
[9] J.L. Feng, B. Fornal, I. Galon, S. Gardner, J. Smolinsky, T.M.P. Tait, P. Tanedo, Phys. Rev. D **95**, 035017 (2017)
[10] C.J.G. Mommers, M. Vanderhaeghen, (to be published) (2023), 2307.02181
[11] L. Doria, P. Achenbach, M. Christmann, A. Denig, H. Merkel, PoS **ALPS2019**, 022 (2020), 1908.07921
[12] B.S. Schlimme et al. (A1, MAGIX), Nucl. Instrum. Meth. A **1013**, 165668 (2021), 2104.13503
[13] H. Merkel et al., Phys. Rev. Lett. **112**, 221802 (2014), 1404.5502
[14] J. Backens, M. Vanderhaeghen, Phys. Rev. Lett. **128**, 091802 (2022)
[15] N.H. Rehbehn, M.K. Rosner, J.C. Berengut, P.O. ~Schmidt, T. Pfeifer, M.F. Gu, J.R. Crespo López-Urrutia, Phys. Rev. Lett. **131**, 161803 (2023), 2309.17141
[16] J.C. Berengut, C. Delaunay, A. Geddes, Y. Soreq, Phys. Rev. Res. **2**, 043444 (2020), 2005.06144
[17] M.I. Levchuk, A.I. L'vov, V.A. Petrunkin, Few Body Syst. **16**, 101 (1994)
[18] R. Machleidt, Phys. Rev. C **63**, 024001 (2001)
[19] D.S.M. Alves, N. Weiner, J. High Energy Phys. **07**, 092 (2018)
[20] J. Kozaczuk, D.E. Morrissey, S.R. Stroberg, Phys. Rev. D **95**, 115024 (2017)
[21] D. Barducci, C. Toni, J. High Energy Phys. **02**, 154 (2023)
[22] P.B. Denton, J. Gehrlein, Phys. Rev. D **108**, 015009 (2023), 2304.09877
[23] M. Hostert, M. Pospelov, Phys. Rev. D **108**, 055011 (2023), 2306.15077
[24] R.L. Workman et al. (Particle Data Group), PTEP **2022**, 083C01 (2022)
[25] T. Beranek, H. Merkel, M. Vanderhaeghen, Phys. Rev. D **88**, 015032 (2013), 1303.2540
[26] R.L. Workman, Others (Particle Data Group), PTEP **2022**, 083C01 (2022)
[27] E. Mornacchi et al. (A2 Collaboration at MAMI), Phys. Rev. Lett. **128**, 132503 (2022), 2110.15691